JPET Fast Forward. Published on December 20, 2017 as DOI: 10.1124/jpet.117.244129
This article has not been copyedited and formatted. The final version may differ from this version.

The Journal of Pharmacology and Experimental Therapeutics

The triple angiokinase inhibitor nintedanib directly inhibits tumor cell growth and induces tumor shrinkage via blocking oncogenic receptor tyrosine kinases

Frank Hilberg, Ulrike Tontsch-Grunt, Anke Baum, Anh T. Le, Robert C. Doebele, Simone Lieb, Davide Gianni, Tilman Voss, Pilar Garin-Chesa, Christian Haslinger and Norbert Kraut

Boehringer Ingelheim RCV GmbH Co KG, Dr. Boehringer-Gasse 5-11, A-1121 Vienna, Austria (F.H., U.T-G, A.B., S.L., D.G., P.G-C, C.H., N.K.)

University of Colorado, School of Medicine, Division of Medical Oncology, 12801 E. 17th Ave., MS 8117, Aurora, CO 80045 (A.T.L., R.C.D.)

AstraZeneca - Innovative Medicines and Early Development | Discovery Sciences, 310 Unit Darwin Building - Cambridge Science Park - Milton Rd - CB4 0WG (D.G.)

Running title: nintedanib small molecule TKI direct inhibition of tumor cell growth

Corresponding author:

Frank Hilberg

Boehringer Ingelheim RCV GmbH Co KG

Dr. Boehringer-Gasse 5-11

A-1121 Vienna, Austria

Phone: ++43-1-80105-2351

Fax: ++43-1-80105-2366

e-mail: frank.hilberg@boehringer-ingelheim.com

manuscript pages : 30

number of tables: 3

number of figures : 4

number of references : 55

Abstract: 248 words

Introduction: 578 words

Discussion: 1200 words

ABBREVIATIONS: KD, knockdown.

Section assignment: Drug discovery and Translational Medicine

Abstract

The triple angiokinase inhibitor nintedanib is an orally available, potent and selective inhibitor of tumor angiogenesis by blocking the tyrosine kinase activities of VEGFR 1-3, PDGFR α and β and FGFR 1-3. Nintedanib has received regulatory approval in second line adenocarcinoma NSCLC in combination with docetaxel. In addition, nintedanib has been approved for the treatment of idiopathic lung fibrosis. Here we report the results from a broad kinase screen that identified additional kinases as targets for nintedanib in the low nanomolar range. Several of these kinases are known to be mutated or overexpressed and are involved in tumor development (DDR1 and 2, TRKA and C, Ret) as well as in fibrotic diseases (eg. DDRs). In tumor cell lines displaying molecular alterations in potential nintedanib targets, the inhibitor demonstrates direct anti-proliferative effects: in the NSCLC cell line NCI-H1703 carrying a PDGFRα amplification; the gastric cancer cell line KatoIII and the breast cancer cell line MFM223 both driven by a FGFR2 amplification; AN3CA (endometrial carcinoma) bearing a mutated FGFR2; the AML cell lines MOLM-13 and MV-4-11-B with FLT3 mutations; the NSCLC adenocarcinoma LC-2/ad harboring a CCDC6-RET fusion. However, potent kinase inhibition does not strictly translate into anti-proliferative activity as demonstrated in the TRKA dependent cell lines CUTO-3 and KM-12. Importantly, nintedanib treatment of NCI-H1703 tumor xenografts triggered effective tumor shrinkage, indicating the direct effect on the tumor cells on top of the antiangiogenic effect on the tumor stroma. These findings will be instructive to guide future genome-based clinical trials with nintedanib.

Introduction

The inhibition of tumor angiogenesis is an established therapeutic option in the treatment of cancer patients. Several small molecule inhibitors as well as antibodies have been approved in recent years starting with bevacizumab in 2004 (Culy, 2005) in CRC and the latest additions of ramucirumab and nintedanib in 2014 (Reinmuth et al., 2015). With the exception of renal cell carcinoma, antiangiogenic treatments are being combined with chemotherapy (Stukalin et al., 2016) (Jayson et al., 2016) to enhance patient response and to prolong overall survival (OS). The mechanism responsible for the enhanced efficacy of chemotherapeutic drugs is still not completely understood, especially since several components of the tumor stroma are involved that are not necessarily linked (Gasparini et al., 2005a; Gasparini et al., 2005b; Boere et al., 2010; Moschetta et al., 2010; Jain, 2014). Hypotheses include tumor vessel normalization through anti-vascular effects leading to better drug delivery and distribution (Jain, 2005; Cesca et al., 2016) and vessel co-option, the ability of tumors to hijack the existing vasculature in organs such as the lungs or liver (Kerbel, 2015). Another possible contribution comes through the inhibition of specific ‘off-target’ kinases of antiangiogenic tyrosine kinase inhibitors (TKIs) that are often associated with the so called multi TKIs (e.g. pazopanib targeting Ret kinase). Nintedanib has been previously described as a triple angiokinase inhibitor targeting the tumor stroma and specifically the vasculature (Hilberg et al., 2008). On the basis of the inhibition profile, nintedanib was profiled as an inhibitor of tumor angiogenesis in clinical trials that led to its regulatory approval in second line adenocarcinoma non-small cell lung cancer (NSCLC) in combination with docetaxel (Reck et al., 2014). Nintedanib shows the strongest benefit in patients with fast progressing tumors that either do not respond to first line platinum based chemotherapy or progress within 6 months after initiation of first line chemo. This hints to a predominant antiangiogenic effect of nintedanib because such fast growing tumors heavily depend on oxygen supply and aerobic metabolism and therefore proper vascular connections (Hilberg et al J Clin Oncol 32, 2014 (suppl; abstr e22080) ASCO poster). The question of whether the extended nintedanib

kinase inhibition profile can contribute to the observed clinical benefit by directly affecting tumor cell proliferation and survival remains pertinent. FGFR genetic alterations such as mutations or amplifications or fusions have been reported for the following cancers: bladder (FGFR3) (Cancer Genome Atlas Research, 2014b), endometrial (FGFR2, (Winterhoff and Konecny, 2016)) and lung (FGFR1, (Weiss et al., 2010; Dienstmann et al., 2014)), breast (FGFR1 and 2), gastric (FGFR2, (Cancer Genome Atlas Research, 2014a)), lung and and glioma (FGFR3-TACC3 fusion; (Capelletti et al., 2014; Di Stefano et al., 2015)). Genetic alterations of the PDGFRA gene occur in about 5% of gastrointestinal stromal tumors (GIST) and amplifications are present in 5-10% of glioblastoma multiforme cases, in oligodendrogliomas, esophageal squamous cell carcinoma, artery intimal sarcomas and in 2-3% NSCLC adenocarcinomas (Heldin, 2013). We here present data that clearly underline the potential of nintedanib to directly inhibit tumor cell proliferation and survival as single agent. This effect of nintedanib can be seen over a wide range of tumor types and various genetic alterations ranging from mutations to amplifications and is also demonstrated in combinations with a small molecule inhibitor targeting a tumor epigenetically. We also demonstrate that inhibition of a RTK at the kinase level does not necessarily translate into a cellular effect. Collectively, our results provide a strong rational for clinical investigations of nintedanib in specific subsets of oncogene-driven cancers.

Methods

Molecular characterization of cancer cell line panel (Ricerca 240-OncoPanel™)

Information on the Ricerca 240-OncoPanel™ can be found at: https://www.eurofinspanlabs.com/Catalog/Products/ProductDetails.aspx?prodId=YWEUPExy%2Fhg%3D and is represented in supplementary Table S3. Relative copy number values were determined using the Affymetrix Genome-Wide Human SNP Array 6.0 platform. The analysis was performed using the CRMA v2 method (Bengtsson et al., 2009), followed by CBS segmentation, both implemented as part of the Aroma Project (http://www.aroma-project.org) (Bengtsson et al., 2008) . Absolute copy numbers were calculated using the PICNIC algorithm (http://www.sanger.ac.uk/science/tools/picnic) (Greenman et al., 2010). Mutation analysis: Mutations were called following best practices as described for instance in (Alioto et al., 2015). RNA-seq data processing and gene expression quantification: Libraries from polyA enrichted RNA (protocols Quiagen, Illumina) were sequenced on an Illumina HiSeq1500 using the Paired-end protocol with 50 cycles and 25 million reads in average. Gene and transcript quantification was performed using SAMtools version 1.0 (Li et al., 2009) and Cufflinks version 2.0.2 (Trapnell et al., 2010). The molecular status of nintedanib target kinases (Table 2) in the Ricerca panel was determined as follows: Kinases with a relative copy number above 4 were considered to be amplified. The threshold for overexpression for each kinase was defined by the respective mean over all cell lines within a tumor type plus 2 times the respective standard deviation. The functional impact of mutations was derived from the MutationAssessor (http://mutationassessor.org/)(Reva et al., 2011) . Statistics calculations (Fisher test) were performed using the R open source programming language (www.r-project.org)(R Core Team (2016) R: A language and environment for statistical computing. R Foundation for Statistical Computing, Vienna, Austria. URL http://www.R-project.org/).

Molecular characteristics of human tumor samples

Gene expression and alteration frequencies (copy number, mutation) within the TCGA data set were analyzed using the cBio Portal online tools (www.cbioportal.org) (Cerami et al., 2012).

Kinase assay

Kinase assays were performed at Thermo Fischer Life Technologies using standard protocols (SelectScreen® Biochemical Profiling Service). ATP concentrations used were at the apparent *Km*.

Z'-LYTE® Assay Conditions: The compounds were screened in 1% DMSO (final concentration) in the well. For 10 point titrations, 3-fold serial dilutions were conducted from the starting concentration. All Peptide/Kinase Mixtures were diluted to a 2x working concentration in the appropriate Kinase Buffer (see section Kinase Specific Assay Conditions for a complete description in supplementary information). All ATP Solutions were diluted to a 4x working concentration in Kinase Buffer (50 mM HEPES pH 7.5, 0.01% BRIJ-35, 10 mM MgCl2, 1 mM EGTA). ATP Km apparent is previously determined using a Z´-LYTE® assay. The Development Reagent is diluted in Development Buffer (see section Kinase-Specific Assay Conditions - Direct and Cascade for a complete description in supplementary information). 10x Novel PKC Lipid Mix: 2 mg/ml Phosphatidyl Serine, 0.2 mg/ml DAG in 20 mM HEPES, pH 7.4, 0.3% CHAPS.

Adapta® Assay Conditions: The compounds wre screened in 1% DMSO (final concentration) in the well. For 10 point titrations, 3-fold serial dilutions are conducted from the starting concentration. All Substrate/Kinase Mixtures were diluted to a 2x working concentration in the appropriate Kinase Buffer (see section Kinase Specific Assay Conditions for a complete description in supplementary information). All ATP Solutions were diluted to a 4x working concentration in water. ATP Km apparent was previously determined using a radiometric assay except when no substrate was available in which case an Adapta® assay was conducted. The Detection Mix was prepared in TR-FRET Dilution Buffer. The Detection mix

consisted of EDTA (30 mM), Eu-anti-ADP antibody (6 nM) and ADP tracer. The detection mix contained the EC60 concentration of tracer for 5-150 µM ATP.

LanthaScreen® Eu Kinase Binding Assay Conditions: The compounds were screened in 1% DMSO (final concentration) in the well. For 10 point titrations, 3-fold serial dilutions were conducted from the starting concentration. All Kinase/Antibody Mixtures were diluted to a 2x working concentration in the appropriate Kinase Buffer (see section Kinase Specific Assay Conditions for a complete description in supplementary information). The 4x AlexaFluor® labeled Tracer was prepared in Kinase Buffer.

Cells and Western blotting

NCI-H1703 cells were seeded in 6-well plates and reverse transfected with 10nmol/l of ON-TARGETplus Human siRNA and Lipofectamin RNAiMAX (Invitrogen #13778075) for 72h at 37°C. Transfections were performed according to the supplier´s manual using the following siRNAs: (FGFR1 siRNA J-003131-00-0002-10; PDGFRA siRNA J-003162-00-0002-12; and Non-targeting siRNA, D-001810-01-20), all obtained from Dharmacon. Two hours prior lysing the cells, nintedanib (BIBF 1120) and/or PD173074 were added in various concentrations to the cultures. Compounds in DMSO were diluted serially and incubated with the cells. Lysates were generated according to standard protocols (Current Protocols in Molecular Biology, edited by F. M. Ausubel, R. Brent, R. E. Kingston, D. D. Moore, J.G. Seidman, J. A. Smith & K. Struhl, 2004, John Wiley and Sons, Inc.). Western blotting was done using standard SDS-PAGE methods, loading 10 µg of protein per lane, with detection by enhanced chemiluminescence. The amount of total and phoshorylated proteins were detected with the corresponding antibodies, purchased and used according to the manufacture´s instruction: Phospho-p44/42 MAPK (Erk1/2) (Thr202/Tyr204) (Cell Signaling #9101); p44/42 MAPK (Erk1/2) (Cell Signaling #9102); Akt (#9272);phosphorylated Akt (Ser473) (#4058); Cleaved Caspase-3 (#9665); FGF Receptor 1 (D8E4) XP® Rabbit mAb (#9740); FGF Receptor 2

(D4H9) (#11835) and PDGF Receptor α(#3164) were all obtained from Cell Signaling. GAPDH was used as a loading control (ab8245, Abcam).

Cell Viability Assay

Between 3000 -10000 cells/well were plated in 96-well flat-bottom microtiter plates and incubated overnight at 37°C in a CO2 incubator with the respective medium. Test compound was added at various concentrations for 72 hours. After 6-hour incubation with Alamar Blue solution (Thermo Fischer / Invitrogen, Carlsbad, CA) at 37°C, fluorescence was measured (Envision MultiModeReader; PerkinElmer) using an excitation wavelength of 531 nm and emission at 595 nm. Data Analysis: Data were fitted by an iterative calculation using a sigmoidal curve analysis program (Prism version 3.0; Graph Pad, La Jolla, CA) with variable hill slope from which EC_{50} values were calculated.

Incucyte Assay

Acute myeloid leukemia (AML) cells (MOLM-13, MV-4-11B, and THP-1) were plated (1 × 10^4/well) in 96-well poly-d-lysine–coated black/clear bottom plates (BD BioCoat). The next day compounds were added at the indicated concentrations. Visualization and measurement of cell growth was by IncuCyte ZOOM® live cell imaging. Cell confluence was monitored for up to 140 hours during which images were taken every 3 hours.

***In vivo* tumor models.**

Mice were housed under pathogen-free conditions (AAALAC accredited facility) and treated according to the institutional, governmental and European Union guidelines (Austrian Animal Protection Laws, GV-SOLAS, FELASA). All animal studies were reviewed and approved by the internal ethics committee and the local governmental committee. Six to eight-week-old female BomTAC:NMRI-*Foxn1^{nu}* mice (21-31 g) were inoculated with 1x 10^6 (in 100 µl) NCI-H1703 or 2.5 x 10^6 MV-4-11-B cells s.c. into the right flank. Tumors were measured three times weekly using calipers. Volumes were calculated according to the formula “tumor

JPET Fast Forward. Published on December 20, 2017 as DOI: 10.1124/jpet.117.244129
This article has not been copyedited and formatted. The final version may differ from this version.

volume = length * diameter2 * π/6." Tumor growth inhibition (TGI) was calculated to the formula: "TGI =100 x {1-[(treated$_{\text{final day}}$– treated$_{\text{day1}}$) / (control$_{\text{final day}}$– control$_{\text{day1}}$)]}"

One-sided decreasing Mann–Whitney tests were used to compare tumor volumes (efficacy). The P values for the tumor volume assessment were adjusted for multiple comparisons according to Bonferroni–Holm. For all analyses, P values under 0.05 represented a statistically significant effect. Kaplan-Meier survival curves were calculated calculation using a curve analysis program (Prism version 3.0; Graph Pad, La Jolla, CA).

Results

Nintedanib shows potent inhibition of FGFR tyrosine kinases 1-3 and PDGFR tyrosine kinases α/β

A head-to-head comparison of nintedanib to in-class competitor molecules revealed that nintedanib is more potent and has a more balanced inhibition profile across the triple angiokinase panel. Nintedanib was compared to sunitinib, vandetanib, pazopanib and cediranib on the basis of the IC_{50} values determined in parallel assays (Table 1). For nintedanib the previously reported potency on VEGFR1-3, PDGFRα and β and on FGFR1-3 could be replicated with IC_{50} values below 100nmol/l with slightly lower IC_{50} values for VEGFR2 and 3 and PDGFRα and β (Hilberg et al., 2008). Sunitinib, vandetanib, pazopanib and cediranib inhibit VEGFR-2 and -3 at concentrations below 100nmol/l, but their inhibition of PDGFR α and β is less potent and there is a clear potency drop with respect to FGFR inhibition. The notable exception is cediranib which exhibits inhibition across the FGFRs which is comparable to nintedanib. In this comparison, sorafenib is the least potent drug with IC_{50} values equal to or higher than 100nmol/l across the tested kinase panel.

Nintedanib potently inhibits oncogenic RTKs beyond FGFRs and PDGFRs

The previously reported kinase target spectrum presented nintedanib as a triple angiokinase small molecule TKI (Hilberg et al., 2008). To explore kinase inhibition beyond that described previously, nintedanib was tested on a much broader, 245 kinase panel. In addition to the 13 kinases that had been previously reported as nintedanib targets, we identified 21 additional kinases that are also inhibited by nintedanib with IC_{50} values below 100nmol/l (Table 2). Among these newly identified targets are kinases well known to be deregulated through genetic alterations and thus may act as oncogenic drivers in human cancers. These include kinases altered in subsets of NSCLC such as Ret (2nmol/l; (Berge and Doebele, 2014) and TRKA (35 nmol/l; (Marchetti et al., 2008). The kinases Abl1 and Kit (13 and 9 nmol/l, respectively) are also known to be driving mutations in several tumour types including

leukemias (Greuber et al., 2013) (Stankov et al., 2014). Nintedanib also inhibits DDR1 and 2 (23 and 18 nmol/l, respectively) which have been described as being involved in inflammatory and fibrotic processes (Guerrot et al., 2011; Olaso et al., 2011).

The fact that TKIs interfere with kinase activity in *in vitro* kinase assays does not necessarily mean that this activity will translate into cellular activity. We addressed this issue in two cell lines with known rearrangements of *NTRK1* leading to constitutive TRKA receptor activation: the CUTO-3.29 NSCLC adenocarcinoma cell line bearing the MPRIP-NTRK1 rearrangement and (Doebele et al., 2015)) and the microsatellite instability (MSI) high colorectal cancer (CRC) cell line KM-12 which has the TPM3-NTRK1 translocation (Camps et al., 2004). As shown in Figure 1, the CUTO-3.29 (Figure 1C) and KM12 (Figure 1D) cells have high levels of pTRKA resulting in elevated pERK1/2 and pAKT levels. As demonstrated, these pTRKA and pERK1/2 levels can be reduced by the addition of the TRK-specific inhibitor, entrectinib, at concentrations as low as 1 nmol/l. In contrast, much higher concetrations of nintedanib ($\geq$1000 nmol/l) were required to reduce pTRKA and pERK1/2 levels. The EC_{50} values of nintedanib and entrectinib were calculated to be 955 nmol/l and 117 nmol/l for the CUTO-3.29 cells and 557 nmol/l and 2.3 nmol/l for the KM12 cell line, respectively (Figure 1A and B). Thus, although nintedanib is a relatively potent inhibitor of TRKA in the kinase panel, this potency does not translate into inhibition of receptor phosphorylation and downstream signaling in cancer cell lines bearing TRKA rearrangements.

Nintedanib inhibits tumor cell proliferation directly

In order to address the cellular inhibitory capacity of nintedanib in more detail the drug was tested on a large collection of cell lines (Ricerca 240-OncoPanel™, supplementary Table S3). Nintedanib displayed efficacy (cutoff: 500 nmol/l, supplementary Table S1a) against 12 of the 242 cancer cell lines across several indications (Figure 2A) including gastric carcinoma, chronic myelogenous leukemia (CML), acute myeloid leukemia (AML), NSCLC, renal cancer, rhabdomyosarcoma and thyroid carcinoma (Supplementary Table S1b). These cell lines

carry driver mutations that may, potentially, be targeted by nintedanib. For example, the AML cell line MV-4-11 expresses the mutated FLT3 ITD allele exclusively which acts as the oncogenic driver (Quentmeier et al., 2003) and which is inhibited by nintedanib with a GI_{50} of 53 nmol/l (supplementary Table S1a). Of the 12 sensitive cell lines, 10 exhibited genetic alterations within a total number of 16 nintedanib target kinases, either as mutation, amplification or overexpression (Figure 2B, Table S2). The two sensitive cell lines that do not carry mutations in any of the nintedanib target kinases are the highly mutated A-427 (NSCLC) line which carryies 418 mutations and the RCC cell line G-401 with 311 mutations (Table S1a). In addition, the A-427 cell line shows a highly complex amplification pattern. The 16 kinase genes as shown in Fig. 2B are altered to a similar extent in both sensitive and insensitive cell lines.

The TCGA data sets for those tumor types represented by the sensitive cell lines was queried to determine the total frequency of alterations in the 16 nintedanib targetable kinases. Around 42 % of gastric cancer cases harbored molecular alterations in any of the described 16 genes. The alterations detected in Acute Myeloid Leukemia and Chronic Lymphatic Leukemia were mostly mutations compared to amplifications or rearrangements (supplementary Figure S1). The kinases overexpressed in the nintedanib sensitive cell lines were, to a certain extent, also overexpressed in the respective TCGA data sets (supplementary Figure S2). In summary, 8 of the 12 nintedanib sensitive cell lines from the 242 cancer panel contained genetic alterations in kinases targeted by nintedanib.

Effects on growth of tumor cell lines in vitro where nintedanib targets may be driver mutations

We determined the responses of the the NSCLC cell line NCI-H1703 (PDGFRα and FGFR1 ampl.), the gastric cancer line KatoIII (FGFR2 ampl.), the endometrial cancer cell line AN3CA (FGFR2 mut.) and the breast cancer cell line MFM-223 (FGFR2 ampl.) to treatment with nintedanib. As shown in Table 1B, growth of all 4 cell lines was inhibited by nintedanib

treatment with EC_{50} values in the lower nanomolar range: NCI-H1703 10 nmol/l, KatoIII 176 nmol/l, AN3CA 152 nmol/l and MFM-223 108 nmol/l. As expected, sorafenib which is a very weak inhibitor of PDGFR and FGFR kinase activity (see Table 1A) was also a weak inhibitor of the NCI-H1703 and Kato III cell lines (EC_{50} values of 258 nmol/l and 383 nmol/l respectively; Table 1B). Sunitinib, which had IC_{50} values of 71 nmol/l and 184 nmol/l against PDGFRα and FGFR2 kinases respectively (Table 1A) was also markedly less potent than nintedanib with EC_{50} values of 39 nmol/l for the NCI-H1703 cells and 624 nmol/l against the KatoIII line (Table 1B). The differences between nintedanib, sunitinib and sorafenib were confirmed by signaling pathway analysis in NCI-H1703 cells following PDGF BB stimulation. As shown in Figure 3D, nintedanib and sunitinib were able to reduce pMAPK, pAKT and pPDGFRα levels in a concentration-dependent manner down to 10-50 nmol/l whereas sorafenib was only able to fully interfere with MAPK, AKT and PDGFRα activation at the highest tested concentration of 1 µmol/l.

Figure 3A also shows that activation of MAPK after stimulation with PDGF BB is inhibited by nintedanib at concentrations of 10 nmol/l and above. The same effect can be seen for phosphorylated AKT. In addition the conversion of PARP to cleaved PARP as a marker of apoptosis is also seen at nintedanib concentrations 30 nmol/l and above. In comparison we also examined the effects of imatinib a TKI that weakly inhibits PDGFR (Capdeville et al., 2002) in this setting. As shown in Figure 3A, imatinib interferes with MAPK and AKT activation only at the highest concentration tested (1,000 nmol/l) resulting in a faint cPARP signal. This difference between nintedanib and imatinib results from the lower (10-fold) potency of imatinib in inhibiting PDGFRB kinase activity which is corroborated by the EC_{50} values of imatinib in comparison to those of nintedanib shown in (Table 1B).

As shown in supplementary Figure S3, both the NCI-H1703 and KatoIII cell lines have two genetic amplifications. PDGFRA and FGFR1 are focally amplified in the NCI-H1703 cells whereas FGFR2 and PDGFRA are amplified in the KatoIII cells. In order to determine which genetic alteration is driving proliferation and survival in these two cell lines, knockdown

experiments were performed. Figure 3B shows that knocking down FGFR1 in the NCI-H1703 cells had no effect on pAKT and pMAPK whereas the PDGFRA knock down (KD) reduced the pMAPK as well as the pAKT signal. The addition of increasing concentrations of nintedanib to the PDGFRA KD resulted in a complete loss of the pMAPK and pAKT signals. The addition of nintedanib to the FGFR1 KD also had an impact on the pAKT and MAPK signals but to a lesser extent demonstrating that NCI-H1703 cells are primarily driven by the PDGFRA amplification.

Among the cancer indications with nintedanib-targetable driver mutations, gastric cancer shows a FGFR2 amplification prevalence of 4-10% (Cancer Genome Atlas Research, 2014a). As a representative from this group we analysed the effects of nintedanib on proliferation and survival pathways in the KatoIII cells. This cell line has been reported to have a copy number gain of 17 for FGFR2. Nintedanib inhibited proliferation in this cell line with an IC_{50} of 176 nmol/l and interfered with MAPK and AKT activation in bFGF stimulated KatoIII cells down to 100 nmol/l and 30 nmol/l, respectively (Figure 3C). In the same experiment, the pan-FGFR inhibitor PD173074 inhibited KatoIII cell proliferation with an IC_{50} of 30 nmol/l and interfered with MAPK and AKT at a concentration as low as 10 nmol/l.

The NSCLC adenocarcinoma cell line LC-2/ad which carries a CCDC6-RET fusion as a driver mutation (Suzuki et al., 2013) was also tested for its response to nintedanib, based on our finding that RET is also a target for the drug (EC_{50} value = 149 nmol/l). In the same experiment vandetanib, a marketed drug for the treatment of thyroid carcinoma based on its Ret inhibition, gave an EC_{50} value of 247 nmol/l (data not shown).

Based on the previously reported inhibition of Flt3 by nintedanib (Kulimova et al., 2006; Hilberg et al., 2008) we were interested in exploring the combination with the small molecule BET (bromodomain and extraterminal) family inhibitor BI 894999 (Effects of the novel BET inhibitor BI 894999 on upregulation of *HEXIM1* in cancer cells and on anti-tumor activity in xenograft tumor models. J Clin Oncol 34, 2016, suppl; abstr 11574 (ASCO)). As

demonstrated in supplementary Figure 4, nintedanib specifically contributes to the inhibition of proliferation in Flt3 mutated AML cell lines (MOLM-13 and MV-4-11-B) but did not inhibit the proliferation of THP-1 AML cells carrying wild type Flt3. The combination of nintedanib with BI 894999 completely inhibited the proliferation of MOLM-13 and MV-4-11-B AML cells, whereas there was no beneficial effect of the combination in the Flt3 wild type cell line (Fiskus et al., 2014).

In vivo anti-tumor efficacy of nintedanib in tumor xenografts bearing nintedanib-targeted driver alterations

As nintedanib potently inhibited *in vitro* growth of the NCI-H1703 NSCLC cell line which bears a PDGFRα amplification we decided to analyze the *in vivo* anti-tumor efficacy in tumor bearing mice. As demonstrated in Figure 4A and B, mice bearing subcutaneous NCI-H1703 tumors were treated with either nintedanib (blocking VEGFR-2 and PDGFRs), vatalanib, a predominantly VEGFR-2 inhibiting TKI, and two different doses of the PDGFR inhibitor imatinib (75 mg/kg qd and bid). The selection of the doses of the drugs for the *in vivo* experiment was based on previously published reports demonstrating exposure of >1µmol/l peak plasma concentrations with the selected doses of 100 mg/kg for nintedanib (Hilberg et al., 2008) and vatalanib (Wood et al., 2000). In accordance with its *in vitro* activity on NCI-H1703 cells nintedanib was the most potent of the 3 compounds in terms of its *in vivo* anti-tumor efficacy resulting in tumor shrinkage with a TGI value of 107% at 100 mg/kg. In comparison, the PDGFR inhibitor imatinib at 75mg/kg either once or twice daily achieved TGI values of 45% and 58%, respectively. Once daily treatment with vatalanib at a dose of 100mg/kg resulted in a TGI of 73%, which is in line with effects observed for anti-angiogenic drugs. All treatments were well tolerated as demonstrated by the weight gain of all treatment groups over the treatment period (data not shown).

The anti-tumor efficacy of nintedanib alone and in combination with the BET family inhibitor BI 894999 was assessed in the subcutaneous MV-4-11-B AML model as shown in Figure 4C,

D and E. The TGI values for the single agent BET inhibitor BI 894999 were 78%, 92% for nintedanib and 99% for the combination. The combination was well tolerated and dosing could be maintained for almost 100 days as also shown in the Kaplan-Meyer plot in Figure 4E. Seven out of eight animals in the combination treatment group survived until the end of the experiment with only one treatment unrelated death. In the BI 894999 treatment group all animals had to be euthanized according to termination criteria at around day 50 and in the nintedanib group five animals were euthanized at day 100.

Discussion

The triple angiokinase inhibitor nintedanib has received regulatory approval for the treatment of idiopathic lung fibrosis as well as for second line NSCLC in combination with docetaxel (Bronte et al., 2016). In this report we present, for the first time, pharmacological evidence that nintedanib directly and potently inhibits growth of tumors that are driven by genetic alterations in nintedanib target kinases. A screen of 240 tumor cell lines revealed 12 nintedanib- sensitive cell lines, nearly half of which were derived from leukemias. The 16 nintedanib-sensitive kinases were either amplified, mutated or overexpressed in these cell lines. None of the mutations represent known functional hotspots in the respective kinase domains and their functional impact is, as yet, unknown. However, the activating nature of mutations outside the kinase domain has for example been demonstrated for PI3 kinase (Kang et al., 2005). The 2 cell lines that did not exhibit mutations in the nintedanib target genes showed multiple mutations and amplification patterns which were too complex to derive clear sensitivity determinants for nintedanib. Alterations to the 16 nintedanib-sensitive kinases are not exclusive to the sensitive cell lines, they are also present in the insensitive cell lines which we assume depend on other alterations and combinations to drive malignant behavior.

The TCGA database was interrogated for a combined aberration incidence for these kinases. The highest percentage (42.2%) was observed for gastric cancer, followed by AML (10 %). FLT4 and PDGFRB are frequently overexpressed in gastric cancer and AML indicating that nintedanib might be useful in the treatment of these particular patient populations.

This is potentially important in a scientific / clinical environment where tumor treatment is becoming increasingly fragmented based on the genetic information acquired through analysis of pre-treatment tumor biopsies. This approach is now well established in the treatment of NSCLC patients bearing EML-ALK or EGFR mutations (Rocco et al., 2016), who receive appropriate TKIs targeting these alterations in the first line setting. Mutational screening of cancer is increasingly becoming incorporated into standard clinical practice requiring an increased need for targeted and well tolerated drugs. As demonstrated in this

report, beyond potently inhibiting tumor angiogenesis, nintedanib also effectively blocks proliferation of tumor cells driven by alterations in PDGFRA, FGFR2, RET and FLT3. We show that this anti-proliferative activity also translates into robust single-agent *in vivo* anti-tumor efficacy upon treatment with nintedanib, including tumor shrinkage.

These results show that nintedanib has a dual mechanism: on the one hand, it suppresses tumor angiogenesis and on the other it interferes directly with tumor cell proliferation, resulting in the induction of apoptosis. This opens up new treatment possibilities for nintedanib in tumor subtypes depending on PDGFRA, FGFR2, RET or FLT3 genetic alterations either alone or in combination with chemotherapy. AML associated with an internal tandem duplication of the *FLT3* gene (*FLT3* ITD mutation) has been reported to occur in about 20% of AML patients (Dohner et al., 2015). It is associated with unfavorable outcome and patients are likely to relapse. A new class of compounds, BET inhibitors, are being intensively investigated preclinically and in phase I trials in AML. Combining the BET inhibitor BI 894999 with nintedanib may lead to improved survival benefit with good tolerability in the FLT3 mutant subgroup of AML. These findings extend a previous report on combining a BET inhibitor with a FLT3 tyrosine kinase inhibitor in an *in vitro* setting (Fiskus et al., 2014).

In clinical practice nintedanib has demonstrated good tolerability and easy patient management. Here we show that nintedanib is a potent and well-balanced triple angiokinase inhibitor in comparison to other in-class competitors. Across the board of VEGFR, PDGFR and FGFR isoforms constituting the triple angiokinase inhibition profile, nintedanib exhibits low nanomolar IC_{50} values whereas competitors such as sunitinib, vandetanib, pazopanib and sorafenib completely lack FGFR activity and are less potent inhibitors of VEGFR1-3 and PDGFR α and β. Despite extending the kinase inhibition profile to 34 kinases as targets for nintedanib, the drug is well tolerated by patients on a daily dosing schedule as compared with in-class drugs that require intermittent dosing regimens to minimize adverse effects (Lee and Motzer, 2015). Furthermore, nintedanib has not been associated with serious side effects such as hand-foot syndrome (Li et al., 2015).

More FGFR selective TKIs (e.g. AZD4547, BGJ398) in cancer treatment have demonstrated promising clinical efficacies in phase 2 clinical trials but are also associated with notable adverse effects such as hand-foot syndrome and serous retinopathy (Katoh, 2016). Hibi et al. have addressed the effects of nintedanib in FGFR1 amplified human lung squamous cell carcinoma cell lines H520 and LK-2 and could demonstrate that nintedanib inhibited the proliferation of FGFR1 CNG-positive LSCC cell lines in association with attenuation of the FGFR1–ERK signaling pathway *in vitro* and *in vivo* (Hibi et al., 2016). These data, together with the results presented in this manuscript demonstrate the potential of nintedanib as a potent inhibitor of cancer cells bearing FGFR alterations (amplifications, mutations) that warrants confirmation in clinical trials investigating nintedanib in cancer patients whose tumors harbor FGFR alterations.

Nintedanib's dual activity as a TKI targeting both genetic alterations in tumor cells (FGFRs and PDGFRs) as well as the tumor stroma by interfering with tumor angiogenesis may represent an advantage over drugs that target specific RTKs more selectively. The importance of normalizing the tumor stromal environment becomes ever more important in the context of the up-coming combinations with immune-checkpoint inhibitors (Hendry et al., 2016). Emerging strong data underscore the importance to improve the immune response by interfering with the VEGF driven negative effects on dendritic cell maturation, T-cell activation, regulatory T cell (Treg) proliferation and promotion of myeloid-derived suppressor cells (MDSCs), as well as interfering with the activated tumor vessels and normalizing the tumor vessel bed (Hendry et al., 2016).

The fact that 34 kinases are inhibited at concentrations below 100 nmol/l identifies nintedanib as a multi TK inhibitor. But this fact is somewhat misleading because mere kinase inhibition does not always translate into inhibitory activity in a cellular context. In this report we clearly showed that the kinase inhibition of NTRK1 with an IC_{50} value of 30 nmol/l did not translate into the cellular inhibition of cell lines harboring a TRKA receptor activation. The same discrepancy between kinase and cellular activity has already been observed for LYN and

LCK kinases with a much weaker cellular activity observed as would have been predicted from the kinase inhibition data (Hilberg et al., 2008).

Nintedanib has demonstrated to be a potent antiangiogenic and antifibrotic drug that has received regulatory approval as an anticancer agent and as an antifibrotic drug for the treatment of second line NSCLC in combination with docetaxel and idiopathic lung fibrosis, respectively. The additional features described in this report, namely the anti-proliferative activity in tumors driven by PDGFR, FGFR, FLT3 and RET alterations, can be seen as a future added value for nintedanib's clinical applications in cancer treatment. Similar approaches are already implemented in clinical practice for lung tumors driven by EML-ALK rearrangements (Blackhall and Cappuzzo, 2016) or RET mutated thyroid carcinomas for crizotinib and vandetanib respectively (Chu et al., 2012). Nintedanib is already being tested clinically in some of these sub-indications with data becoming available in the coming years (e.g. NCT02278978, NCT02299141).

Acknowledgements

We are grateful to Monika Kriz, Matthew Kennedy, Martina Scherer, Regina Ruzicka, Nina Rodi, Susanne Schmittner and Susy Straubinger for excellent technical assistance and data evaluation and to Dr. Elizabeth Anderson for critical reading the manuscript.

Authorship Contribution:

Participated in the research design: Hilberg, Tontsch-Grunt, Baum, Le, Doebele, Lieb, Gianni, Voss, Garin-Chesa, Haslinger, Kraut

Conducted experiments: Tontsch-Grunt, Baum, Le, Lieb, Gianni, Voss

Performed data analysis: Hilberg, Tontsch-Grunt, Baum, Le, Doebele, Lieb, Gianni, Voss, Garin-Chesa, Haslinger

Wrote or contributed to the writing of the manuscript: Hilberg, Tontsch-Grunt, Baum, Le, Doebele, Lieb, Gianni, Voss, Garin-Chesa, Haslinger, Kraut

References

Alioto TS, Buchhalter I, Derdak S, Hutter B, Eldridge MD, Hovig E, Heisler LE, Beck TA, Simpson JT, Tonon L, Sertier AS, Patch AM, Jager N, Ginsbach P, Drews R, Paramasivam N, Kabbe R, Chotewutmontri S, Diessl N, Previti C, Schmidt S, Brors B, Feuerbach L, Heinold M, Grobner S, Korshunov A, Tarpey PS, Butler AP, Hinton J, Jones D, Menzies A, Raine K, Shepherd R, Stebbings L, Teague JW, Ribeca P, Giner FC, Beltran S, Raineri E, Dabad M, Heath SC, Gut M, Denroche RE, Harding NJ, Yamaguchi TN, Fujimoto A, Nakagawa H, Quesada V, Valdes-Mas R, Nakken S, Vodak D, Bower L, Lynch AG, Anderson CL, Waddell N, Pearson JV, Grimmond SM, Peto M, Spellman P, He M, Kandoth C, Lee S, Zhang J, Letourneau L, Ma S, Seth S, Torrents D, Xi L, Wheeler DA, Lopez-Otin C, Campo E, Campbell PJ, Boutros PC, Puente XS, Gerhard DS, Pfister SM, McPherson JD, Hudson TJ, Schlesner M, Lichter P, Eils R, Jones DT and Gut IG (2015) A comprehensive assessment of somatic mutation detection in cancer using whole-genome sequencing. *Nat Commun* **6**:10001.

Bengtsson H, Irizarry R, Carvalho B and Speed TP (2008) Estimation and assessment of raw copy numbers at the single locus level. *Bioinformatics* **24**:759-767.

Bengtsson H, Wirapati P and Speed TP (2009) A single-array preprocessing method for estimating full-resolution raw copy numbers from all Affymetrix genotyping arrays including GenomeWideSNP 5 & 6. *Bioinformatics* **25**:2149-2156.

Berge EM and Doebele RC (2014) Targeted therapies in non-small cell lung cancer: emerging oncogene targets following the success of epidermal growth factor receptor. *Semin Oncol* **41**:110-125.

Blackhall F and Cappuzzo F (2016) Crizotinib: from discovery to accelerated development to front-line treatment. *Ann Oncol* **27 Suppl 3**:iii35-iii41.

Boere IA, Hamberg P and Sleijfer S (2010) It takes two to tango: combinations of conventional cytotoxics with compounds targeting the vascular endothelial growth factor-vascular endothelial growth factor receptor pathway in patients with solid malignancies. *Cancer Sci* **101**:7-15.

Bronte G, Passiglia F, Galvano A, Barraco N, Listi A, Castiglia M, Rizzo S, Fiorentino E, Bazan V and Russo A (2016) Nintedanib in NSCLC: evidence to date and place in therapy. *Ther Adv Med Oncol* **8**:188-197.

Camps J, Morales C, Prat E, Ribas M, Capella G, Egozcue J, Peinado MA and Miro R (2004) Genetic evolution in colon cancer KM12 cells and metastatic derivates. *Int J Cancer* **110**:869-874.

Cancer Genome Atlas Research N (2014a) Comprehensive molecular characterization of gastric adenocarcinoma. *Nature* **513**:202-209.

Cancer Genome Atlas Research N (2014b) Comprehensive molecular characterization of urothelial bladder carcinoma. *Nature* **507**:315-322.

Capdeville R, Buchdunger E, Zimmermann J and Matter A (2002) Glivec (STI571, imatinib), a rationally developed, targeted anticancer drug. *Nat Rev Drug Discov* **1**:493-502.

Capelletti M, Dodge ME, Ercan D, Hammerman PS, Park SI, Kim J, Sasaki H, Jablons DM, Lipson D, Young L, Stephens PJ, Miller VA, Lindeman NI, Munir KJ, Richards WG and Janne PA (2014) Identification of recurrent FGFR3-TACC3 fusion oncogenes from lung adenocarcinoma. *Clin Cancer Res* **20**:6551-6558.

Cerami E, Gao J, Dogrusoz U, Gross BE, Sumer SO, Aksoy BA, Jacobsen A, Byrne CJ, Heuer ML, Larsson E, Antipin Y, Reva B, Goldberg AP, Sander C and Schultz N (2012) The cBio cancer genomics portal: an open platform for exploring multidimensional cancer genomics data. *Cancer Discov* **2**:401-404.

Cesca M, Morosi L, Berndt A, Fuso Nerini I, Frapolli R, Richter P, Decio A, Dirsch O, Micotti E, Giordano S, D'Incalci M, Davoli E, Zucchetti M and Giavazzi R (2016) Bevacizumab-Induced Inhibition of Angiogenesis Promotes a More Homogeneous Intratumoral Distribution of Paclitaxel, Improving the Antitumor Response. *Mol Cancer Ther* **15**:125-135.

Chu CT, Sada YH and Kim ES (2012) Vandetanib for the treatment of lung cancer. *Expert Opin Investig Drugs* **21**:1211-1221.

Culy C (2005) Bevacizumab: antiangiogenic cancer therapy. *Drugs Today (Barc)* **41**:23-36.

Di Stefano AL, Fucci A, Frattini V, Labussiere M, Mokhtari K, Zoppoli P, Marie Y, Bruno A, Boisselier B, Giry M, Savatovsky J, Touat M, Belaid H, Kamoun A, Idbaih A, Houillier C, Luo FR, Soria JC, Tabernero J, Eoli M, Paterra R, Yip S, Petrecca K, Chan JA, Finocchiaro G, Lasorella A, Sanson M and Iavarone A (2015) Detection, Characterization, and Inhibition of FGFR-TACC Fusions in IDH Wild-type Glioma. *Clin Cancer Res* **21**:3307-3317.

Dienstmann R, Rodon J, Prat A, Perez-Garcia J, Adamo B, Felip E, Cortes J, Iafrate AJ, Nuciforo P and Tabernero J (2014) Genomic aberrations in the FGFR pathway: opportunities for targeted therapies in solid tumors. *Ann Oncol* **25**:552-563.

Doebele RC, Davis LE, Vaishnavi A, Le AT, Estrada-Bernal A, Keysar S, Jimeno A, Varella-Garcia M, Aisner DL, Li Y, Stephens PJ, Morosini D, Tuch BB, Fernandes M, Nanda N and Low JA (2015) An Oncogenic NTRK Fusion in a Patient with Soft-Tissue Sarcoma with Response to the Tropomyosin-Related Kinase Inhibitor LOXO-101. *Cancer Discov* **5**:1049-1057.

Dohner H, Weisdorf DJ and Bloomfield CD (2015) Acute Myeloid Leukemia. *N Engl J Med* **373**:1136-1152.

Fiskus W, Sharma S, Qi J, Shah B, Devaraj SG, Leveque C, Portier BP, Iyer S, Bradner JE and Bhalla KN (2014) BET protein antagonist JQ1 is synergistically lethal with FLT3 tyrosine kinase inhibitor (TKI) and overcomes resistance to FLT3-TKI in AML cells expressing FLT-ITD. *Mol Cancer Ther* **13**:2315-2327.

Gasparini G, Longo R, Fanelli M and Teicher BA (2005a) Combination of antiangiogenic therapy with other anticancer therapies: results, challenges, and open questions. *J Clin Oncol* **23**:1295-1311.

Gasparini G, Longo R, Toi M and Ferrara N (2005b) Angiogenic inhibitors: a new therapeutic strategy in oncology. *Nat Clin Pract Oncol* **2**:562-577.

Greenman CD, Bignell G, Butler A, Edkins S, Hinton J, Beare D, Swamy S, Santarius T, Chen L, Widaa S, Futreal PA and Stratton MR (2010) PICNIC: an algorithm to predict absolute allelic copy number variation with microarray cancer data. *Biostatistics* **11**:164-175.

Greuber EK, Smith-Pearson P, Wang J and Pendergast AM (2013) Role of ABL family kinases in cancer: from leukaemia to solid tumours. *Nat Rev Cancer* **13**:559-571.

Guerrot D, Kerroch M, Placier S, Vandermeersch S, Trivin C, Mael-Ainin M, Chatziantoniou C and Dussaule JC (2011) Discoidin domain receptor 1 is a major mediator of inflammation and fibrosis in obstructive nephropathy. *Am J Pathol* **179**:83-91.

Heldin CH (2013) Targeting the PDGF signaling pathway in tumor treatment. *Cell Commun Signal* **11**:97.

Hendry SA, Farnsworth RH, Solomon B, Achen MG, Stacker SA and Fox SB (2016) The Role of the Tumor Vasculature in the Host Immune Response: Implications for Therapeutic Strategies Targeting the Tumor Microenvironment. *Front Immunol* **7**:621.

Hibi M, Kaneda H, Tanizaki J, Sakai K, Togashi Y, Terashima M, De Velasco MA, Fujita Y, Banno E, Nakamura Y, Takeda M, Ito A, Mitsudomi T, Nakagawa K, Okamoto I and Nishio K (2016) FGFR gene alterations in lung squamous cell carcinoma are potential targets for the multikinase inhibitor nintedanib. *Cancer Sci* **107**:1667-1676.

Hilberg F, Roth GJ, Krssak M, Kautschitsch S, Sommergruber W, Tontsch-Grunt U, Garin-Chesa P, Bader G, Zoephel A, Quant J, Heckel A and Rettig WJ (2008) BIBF 1120: triple angiokinase inhibitor with sustained receptor blockade and good antitumor efficacy. *Cancer Res* **68**:4774-4782.

Jain RK (2005) Antiangiogenic therapy for cancer: current and emerging concepts. *Oncology (Williston Park)* **19**:7-16.

Jain RK (2014) Antiangiogenesis strategies revisited: from starving tumors to alleviating hypoxia. *Cancer Cell* **26**:605-622.

Jayson GC, Kerbel R, Ellis LM and Harris AL (2016) Antiangiogenic therapy in oncology: current status and future directions. *Lancet* **388**:518-529.

Kang S, Bader AG and Vogt PK (2005) Phosphatidylinositol 3-kinase mutations identified in human cancer are oncogenic. *Proc Natl Acad Sci U S A* **102**:802-807.

Katoh M (2016) FGFR inhibitors: Effects on cancer cells, tumor microenvironment and whole-body homeostasis (Review). *Int J Mol Med* **38**:3-15.

Kerbel RS (2015) A Decade of Experience in Developing Preclinical Models of Advanced- or Early-Stage Spontaneous Metastasis to Study Antiangiogenic Drugs, Metronomic Chemotherapy, and the Tumor Microenvironment. *Cancer J* **21**:274-283.

Kulimova E, Oelmann E, Bisping G, Kienast J, Mesters RM, Schwable J, Hilberg F, Roth GJ, Munzert G, Stefanic M, Steffen B, Brandts C, Muller-Tidow C, Kolkmeyer A, Buchner T, Serve H and Berdel WE (2006) Growth inhibition and induction of apoptosis in acute myeloid leukemia cells by new indolinone derivatives targeting fibroblast growth factor, platelet-derived growth factor, and vascular endothelial growth factor receptors. *Mol Cancer Ther* **5**:3105-3112.

Lee CH and Motzer RJ (2015) Sunitinib as a paradigm for tyrosine kinase inhibitor development for renal cell carcinoma. *Urol Oncol* **33**:275-279.

Li H, Handsaker B, Wysoker A, Fennell T, Ruan J, Homer N, Marth G, Abecasis G, Durbin R and Genome Project Data Processing S (2009) The Sequence Alignment/Map format and SAMtools. *Bioinformatics* **25**:2078-2079.

Li Y, Gao ZH and Qu XJ (2015) The adverse effects of sorafenib in patients with advanced cancers. *Basic Clin Pharmacol Toxicol* **116**:216-221.

Marchetti A, Felicioni L, Pelosi G, Del Grammastro M, Fumagalli C, Sciarrotta M, Malatesta S, Chella A, Barassi F, Mucilli F, Camplese P, D'Antuono T, Sacco R and Buttitta F (2008) Frequent mutations in the neurotrophic tyrosine receptor kinase gene family in large cell neuroendocrine carcinoma of the lung. *Hum Mutat* **29**:609-616.

Moschetta M, Cesca M, Pretto F and Giavazzi R (2010) Angiogenesis inhibitors: implications for combination with conventional therapies. *Curr Pharm Des* **16**:3921-3931.

Olaso E, Lin HC, Wang LH and Friedman SL (2011) Impaired dermal wound healing in discoidin domain receptor 2-deficient mice associated with defective extracellular matrix remodeling. *Fibrogenesis Tissue Repair* **4**:5.

Quentmeier H, Reinhardt J, Zaborski M and Drexler HG (2003) FLT3 mutations in acute myeloid leukemia cell lines. *Leukemia* **17**:120-124.

Reck M, Kaiser R, Mellemgaard A, Douillard JY, Orlov S, Krzakowski M, von Pawel J, Gottfried M, Bondarenko I, Liao M, Gann CN, Barrueco J, Gaschler-Markefski B, Novello S and Group LU-LS (2014) Docetaxel plus nintedanib versus docetaxel plus placebo in patients with previously treated non-small-cell lung cancer (LUME-Lung 1): a phase 3, double-blind, randomised controlled trial. *Lancet Oncol* **15**:143-155.

Reinmuth N, Heigener D and Reck M (2015) Novel angiogenesis inhibitors in nonsmall cell lung cancer. *Curr Opin Oncol* **27**:79-86.

Reva B, Antipin Y and Sander C (2011) Predicting the functional impact of protein mutations: application to cancer genomics. *Nucleic Acids Res* **39**:e118.

Rocco G, Morabito A, Leone A, Muto P, Fiore F and Budillon A (2016) Management of non-small cell lung cancer in the era of personalized medicine. *Int J Biochem Cell Biol* **78**:173-179.

Stankov K, Popovic S and Mikov M (2014) C-KIT signaling in cancer treatment. *Curr Pharm Des* **20**:2849-2880.

Stukalin I, Alimohamed N and Heng DY (2016) Contemporary Treatment of Metastatic Renal Cell Carcinoma. *Oncol Rev* **10**:295.

Suzuki M, Makinoshima H, Matsumoto S, Suzuki A, Mimaki S, Matsushima K, Yoh K, Goto K, Suzuki Y, Ishii G, Ochiai A, Tsuta K, Shibata T, Kohno T, Esumi H and Tsuchihara K (2013) Identification of a lung adenocarcinoma cell line with CCDC6-RET fusion gene and the effect of RET inhibitors in vitro and in vivo. *Cancer Sci* **104**:896-903.

Trapnell C, Williams BA, Pertea G, Mortazavi A, Kwan G, van Baren MJ, Salzberg SL, Wold BJ and Pachter L (2010) Transcript assembly and quantification by RNA-Seq reveals unannotated transcripts and isoform switching during cell differentiation. *Nat Biotechnol* **28**:511-515.

Weiss J, Sos ML, Seidel D, Peifer M, Zander T, Heuckmann JM, Ullrich RT, Menon R, Maier S, Soltermann A, Moch H, Wagener P, Fischer F, Heynck S, Koker M, Schottle J, Leenders F, Gabler F, Dabow I, Querings S, Heukamp LC, Balke-Want H, Ansen S, Rauh D, Baessmann I, Altmuller J, Wainer Z, Conron M, Wright G, Russell P, Solomon B, Brambilla E, Brambilla C, Lorimier P, Sollberg S, Brustugun OT, Engel-Riedel W, Ludwig C, Petersen I, Sanger J, Clement J, Groen H, Timens W, Sietsma H, Thunnissen E, Smit E, Heideman D, Cappuzzo F, Ligorio C, Damiani S, Hallek M, Beroukhim R, Pao W, Klebl B, Baumann M, Buettner R, Ernestus K, Stoelben E, Wolf J, Nurnberg P, Perner S and Thomas RK (2010) Frequent and focal FGFR1 amplification associates with therapeutically tractable FGFR1 dependency in squamous cell lung cancer. *Sci Transl Med* **2**:62ra93.

Winterhoff B and Konecny GE (2016) Targeting fibroblast growth factor pathways in endometrial cancer. *Curr Probl Cancer*.

Wood JM, Bold G, Buchdunger E, Cozens R, Ferrari S, Frei J, Hofmann F, Mestan J, Mett H, O'Reilly T, Persohn E, Rosel J, Schnell C, Stover D, Theuer A, Towbin H, Wenger F, Woods-Cook K, Menrad A, Siemeister G, Schirner M, Thierauch KH, Schneider MR, Drevs J, Martiny-Baron G and Totzke F (2000) PTK787/ZK 222584, a novel and potent inhibitor of vascular endothelial growth factor receptor tyrosine kinases, impairs vascular endothelial growth factor-induced responses and tumor growth after oral administration. *Cancer Res* **60**:2178-2189.

Footnotes:

The authors declare no potential conflicts of interest. FH, UT-G, AB, SL, DG, TV, PG-C, CH and NK are employees of Boehringer Ingelheim.

Reprint requests: Frank Hilberg, Boehringer Ingelheim RCV GmbH Co KG, Dr. Boehringer-Gasse 5-11, A-1121 Vienna, Austria, Phone: ++43-1-80105-2351, Fax: ++43-1-80105-2366
e-mail: frank.hilberg@boehringer-ingelheim.com

Figure Legends

Figure 1. Inhibition of Proliferation and TRKA and downstream signaling of TRKA fusion cell lines using nintedanib and entrectinib. Human TRKA fusion cell lines CUTO3.29 (A) and KM12 (B) were treated with the indicated dose range of ninitedanib (blue) or entrectinib (red) and assayed for cell proliferation 72 hours after treatment using an MTS assay (n = 3, error bars represent ± S.E.M.). The half-maximal inhibitory concentration (IC_{50}) was calculated for each cell line as follow: CUTO3.29 treated with nintedanib, 954.9 ± 7.2 nmol/l or with entrectinib, 117.48 ± 5.6 nmol/l; KM12 treated with nintedanib, 557.1 ± 5.6 nmol/l, and with entrectinib, 2.28 ± 0.3 nmol/l. CUTO3.29 (C) and KM12 (D) were treated with the indicated increasing doses of either nintedanib or entrectinib and protein lysates were collected 2 hours later for western blot analysis of phospho-TRKA and downstream signaling of phospho-ERK1/2, phospho-AKT and phospho-STAT3. Western blot images are representative of 3 independent experiments.

Figure 2. Mutational analysis of nintedanib sensitive tumor cell lines. A: Response of Ricerca 240-OncoPanel™ cell lines to nintedanib. Sensitive cell lines ($GI_{50} \leq 500$ nmol/l) are marked with *. The color code legend highlights the tumor types represented by the sensitive cell lines. B: Venn diagram showing the 16 genes and their respective alterations in the sensitive cell lines highlighted in panel A.

Figure 3. Nintedanib inhibits ligand-dependent phosphorylation of MAPK and Akt in NCI-H1703 and Kato III tumor cells. A: NCI-H1703 Western blot analysis after exposure to either nintedanib or imatinib following stimulation with PDGF BB. Strong concentration-dependent reduction of phosphorylated MAPK and Akt levels by nintedanib as compared to imatinib. B: NCI-H1703 Western blot analysis after 72h of either FGFR1 or PDGFRA siRNA treatment and 2h of exposure to nintedanib shows concentration-dependent reduction of phosphorylated MAPK and Akt levels. Cleaved PARP and cleaved Caspase-3 serve as

indicators for apoptosis. Nintedanib concentrations are shown in µmol/L. C: Kato III Western blot analysis after exposure to either nintedanib or following stimulation with bFGF. Slightly stronger concentration-dependent reduction of phosphorylated MAPK and Akt levels by PD173074 as compared to nintedanib. Western blot images are representative of 3 independent experiments. D: NCI-H1703 Western blot analysis after exposure to either nintedanib, sunitinib or sorafenib following stimulation with PDGF BB. Concentration-dependent reduction of phosphorylated MAPK, Akt and phosphor PDGFRα levels by nintedanib and sunitinib as compared to sorafenib.

Figure 4. Single agent nintedanib induces tumor shrinkage of subcutaneous NCI-H1703 tumors. A) Median tumor volume over time, B) Single tumor volumes + median at day 29, nintedanib, 100 mg/kg qd (open triangles), vatalanib, 100 mg/kg qd (stars), imatinib, 75 mg/kg qd (filled triangles) and imatinib, 75 mg/kg bid (filled diamonds) (n=7). Nintedanib in combination with the BET inhibitor BI894999 shows excellent anti-tumor efficacy with 7 of 8 animals surviving $\geqslant$ 100 days. C) Median tumor volume over time. (Nintedanib treated animals euthanized prematurely because of tumor necrosis.) D) Single tumor volumes + median at day 33. E) Survival probability (n=8 for treatment, n=10 for vehicle control). Xenografts were established s.c. in athymic mice and allowed to reach a volume of ~100 mm^3 before treatment

JPET Fast Forward. Published on December 20, 2017 as DOI: 10.1124/jpet.117.244129
This article has not been copyedited and formatted. The final version may differ from this version.

Table 1A, **Potent inhibition of triple angiokinase targets by nintedanib and competitor compounds**

Kinase *§*	**VEGFR**			**PDGFR**		**FGFR**			
IC_{50} [nmol/l]	**-1**	**-2**	**-3**	**alpha**	**beta**	**-1**	**-2**	**-3**	**-4**
nintedanib	99	3	4	18	28	41	47	96	421
sunitinib	629	96	63	71	38	531	184	559	2670
sorafenib	765	100	274	174	1110	>10000	994	>10000	>10000
vandetanib	208	12	74	187	3190	804	149	970	9560
pazopanib	171	19	94	173	62	321	353	904	1660
cediranib	64	4	18	296	496	39	20	63	622

Performed at Invitrogen, [ATP] @ Km app

§ additional kinases tested: ABL1, ACVR1B (ALK4), AKT2 (PKB beta), AMPK A1/B1/G1, AURKA (Aurora A), CAMK1D (CaMKI delta), CDK2/cyclin A, CHEK1 (CHK1), CSNK1A1 (CK1 alpha 1), CSNK2A1 (CK2 alpha 1), EGFR (ErbB1), EPHB2, FGFR1, FRAP1 (mTOR), GSK3B (GSK3 beta), IGF1R, LCK, MAP2K1 (MEK1), MAP3K8 (COT), MAPK14 (p38 alpha), MAPKAPK2, MYLK2 (skMLCK), NEK2, PAK4, PDK1, PRKACA (PKA), RAF1 (cRAF) Y340D Y341D, ROCK2, SRPK2, STK3 (MST2), TBK1

Table 1B, **Nintedanib potently inhibits the proliferation of cell lines carrying alterations in PDGFRA or FGFR2**

EC_{50} [nmol/l]	**NCI-1703** PDGFRA ampl	**KatoIII** FGFR2 ampl	**AN3CA** FGFR2 mut	**MFM-223** FGFR2 ampl
nintedanib	10 ± 3	176 ± 40	152 ± 22	108
PD173074	n.a.	30 ± 5	n.a.	n.a.
imatinib	109 ± 65	n.a.	n.a.	n.a.
sunitinib	39 ± 10	624 ± 85	n.a.	n.a.
sorafenib	258 ± 25	383 ± 24	n.a.	n.a.

Data were determined using an alamarBlue® Cell Viability Assay Protocol from the Cell Proliferation Assay Protocols section of Life Technologies, drug exposure for 72 h

Table 2: **Extended *in vitro* kinase inhibition profile of nintedanib**

Kinase	**IC_{50} (nmol/L)**
ABL1	12 ± 5
BLK	42 ± 9
BTK	34 ± 14
CSF1R	5 ± 2
DDR1	17 ± 7
DDR2	16 ± 4
FYN	74 ± 24
JAK3	67 ± 27
KIT	6 ± 3
MAP3K3 (MEKK3)	58 ± 25
MAP3K7	46 ± 31
MELK	3 ± 2
MST4	84 ± 9
NTRK1 (TRKA)	30 ± 8
NTRK3 (TRKC)	48 ± 25
NUAK1	50 ± 8
RET	2 ± 1
SIK2	11 ± 4
STK24	61 ± 12
TGFBR1	77 ± 20
YES1	14 ± 4

Data were determined using the SelectScreen® Biochemical Kinase Profiling Service and performed at ThermoFisher/life technologies. Measurements were performed in triplicates. *[ATP] @ Km app*

Hilberg et al., Figure 1

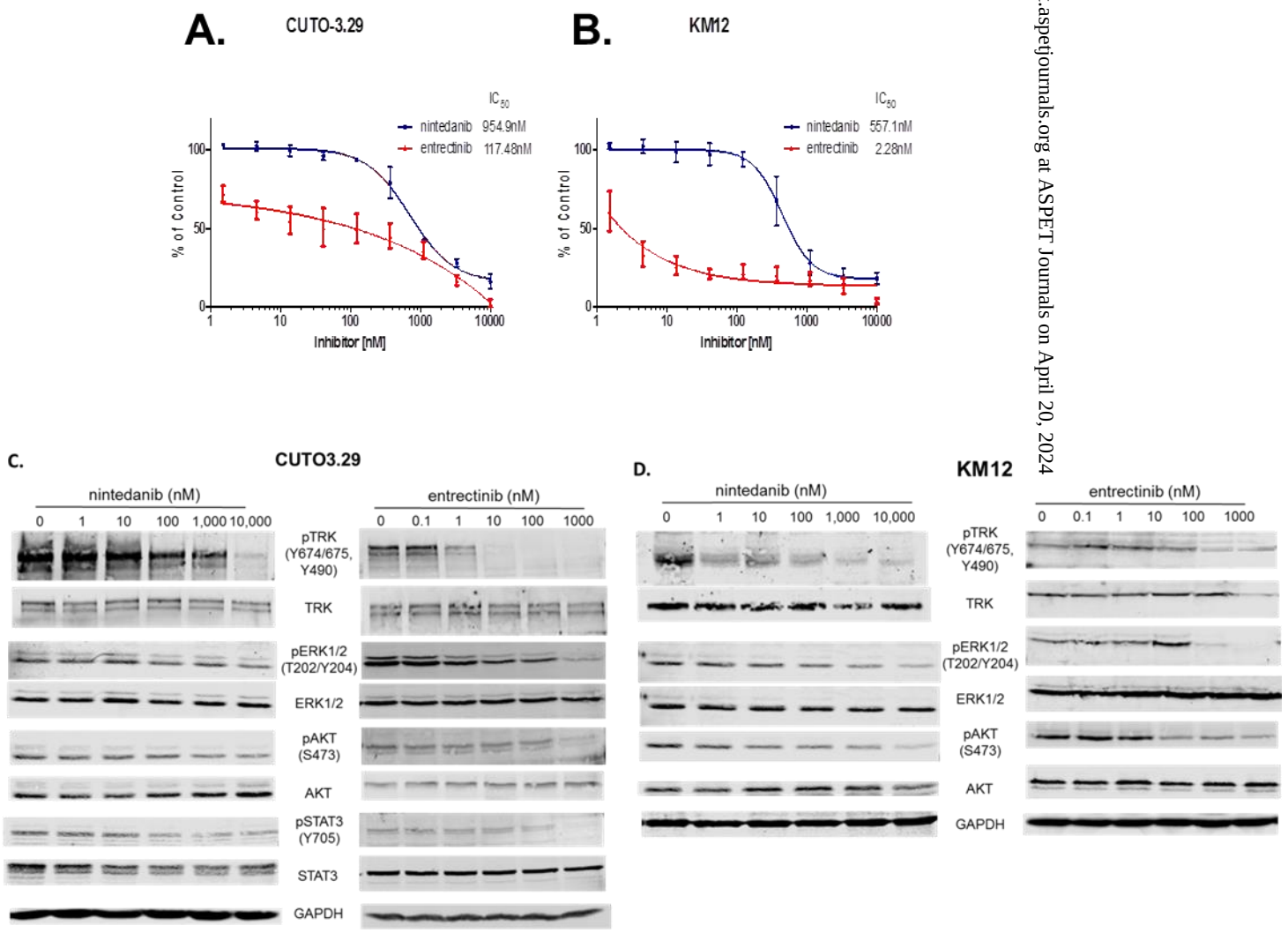

Hilberg et al., Figure 2

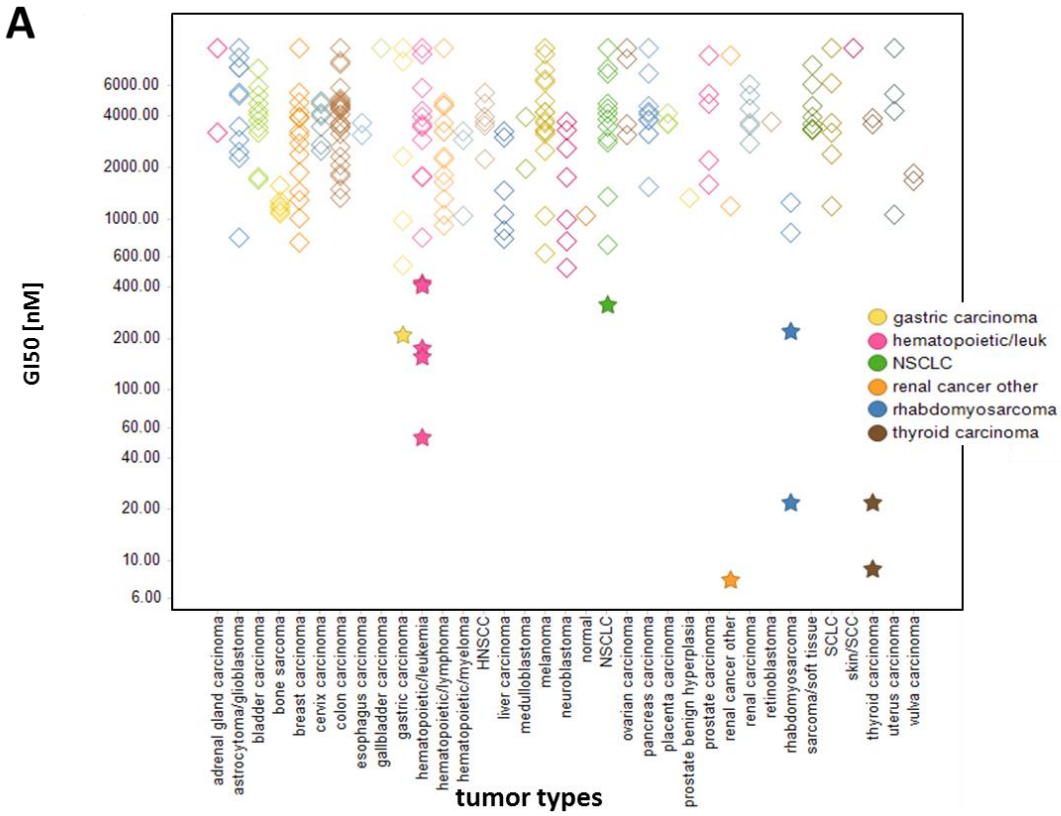

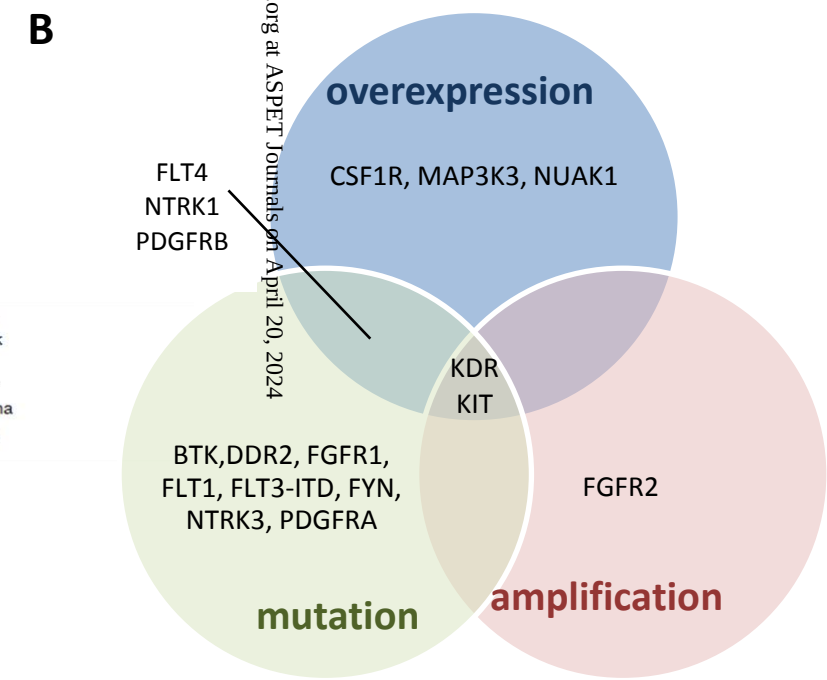

Hilberg et al., Figure 3A

A

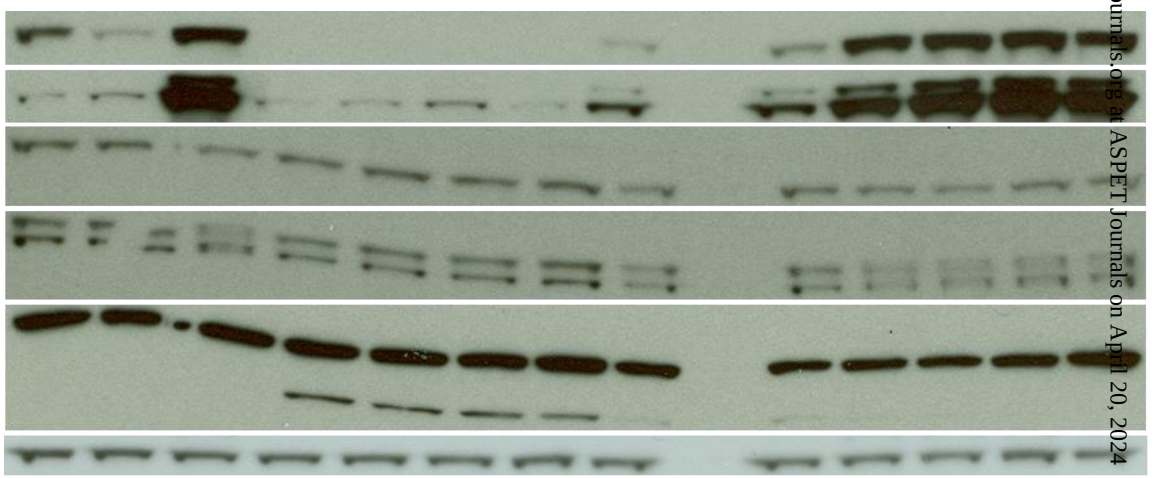

10	0.1	0.1	0.1	0.1	0.1	0.1	0.1	0.1	0.1	0.1	0.1	0.1	*FCS [%]*
-	-	+	+	+	+	+	+	+	+	+	+	+	*PDGF BB*
-	-	-	1	0.3	0.1	0.03	0.01	-	-	-	-	-	*[µM] Nintedanib*
-	-	-	-	-	-	-	-	1	0.3	0.1	0.03	0.01	*[µM] Imatinib*

Hilberg et al., Figure 3B

B

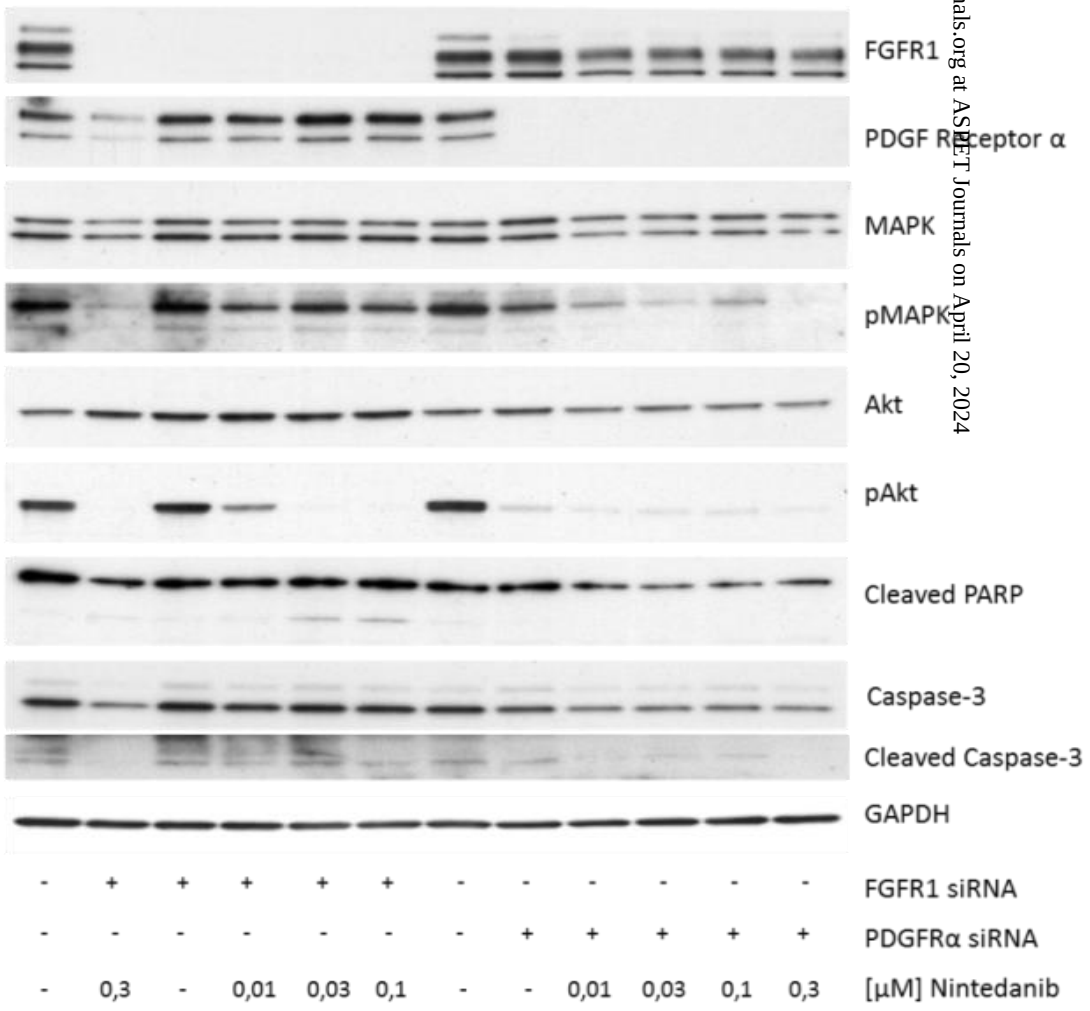

Hilberg et al., Figure 3C

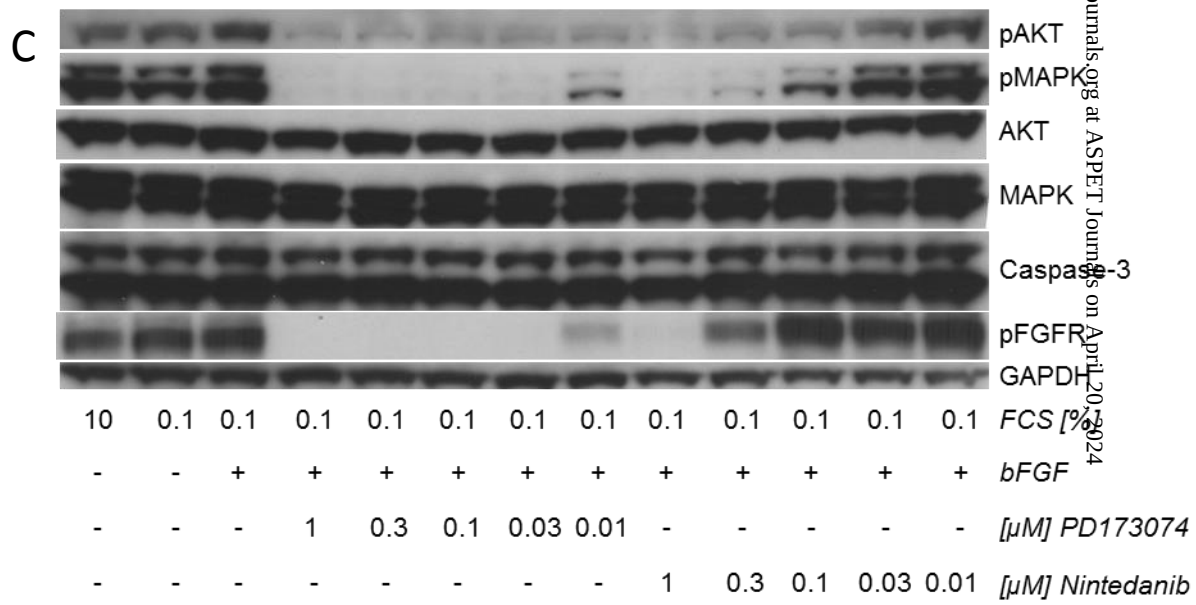

Hilberg et al., Figure 3D

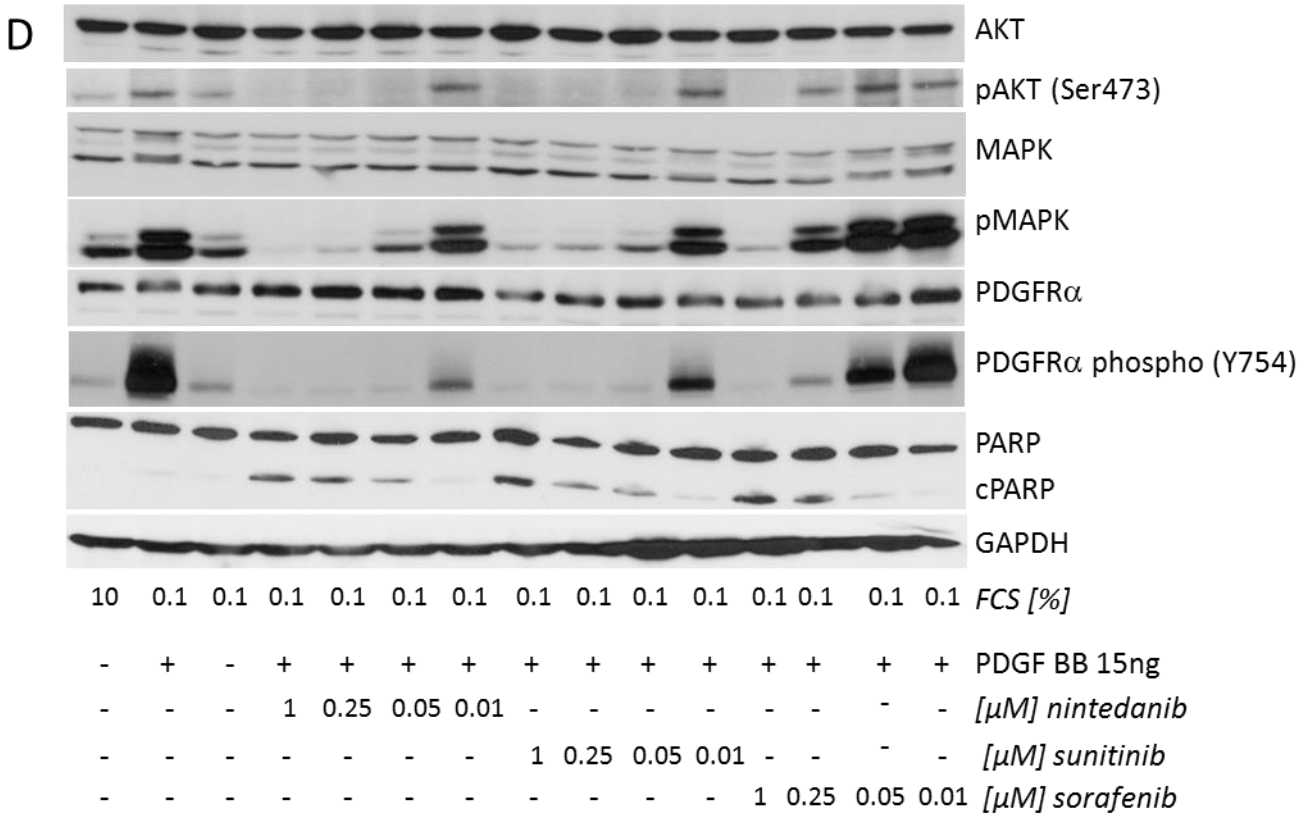

Hilberg et al., Figure 4

A

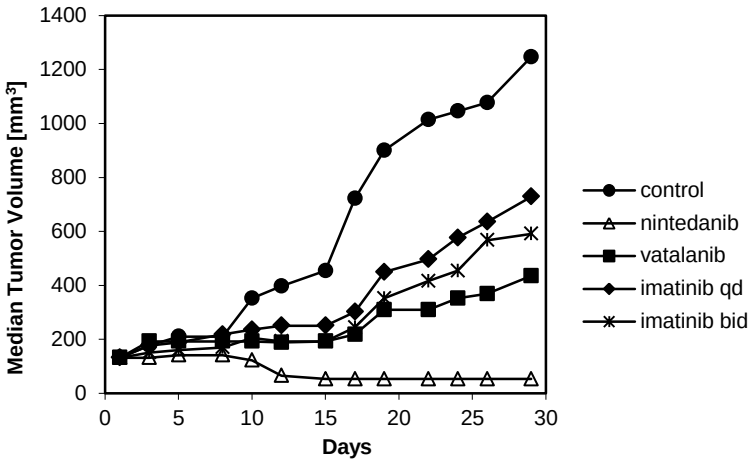

B

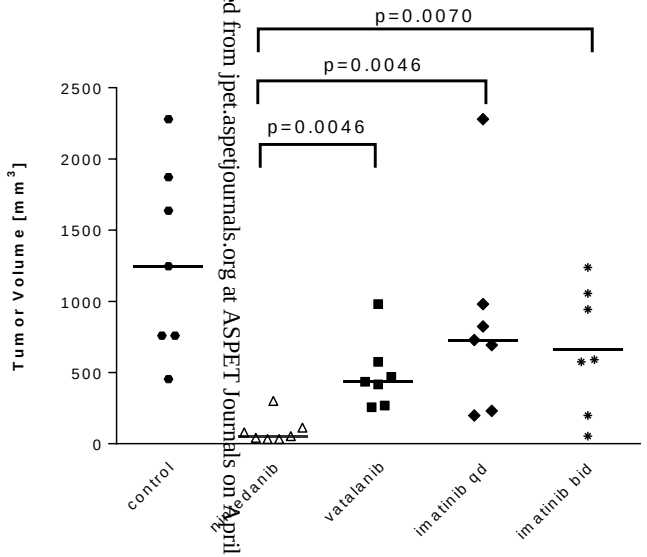

C

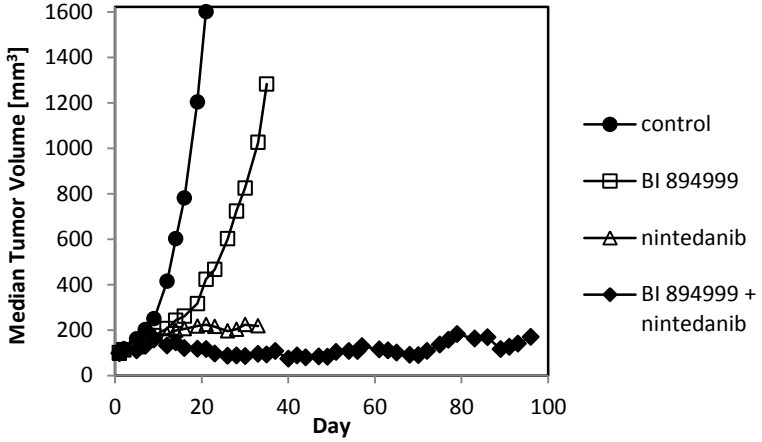

D

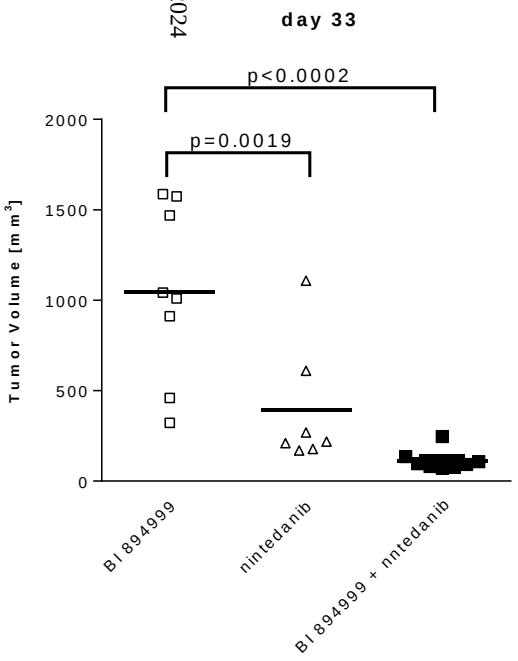

E